

# Measurements of the position-dependent photo-detection sensitivity of the Hamamatsu R11410 and R8520 photomultiplier tubes

---

**L. Baudis, S. D'Amato\*, G. Kessler, A. Kish, J. Wulf**

*Physik-Institut, Universität Zürich,  
Winterthurerstr. 190, CH-8057, Switzerland*

**ABSTRACT:** The Hamamatsu R11410 and R8520 photomultiplier tubes (PMTs) are designed for applications in dark matter detectors using liquid xenon, featuring excellent sensitivity to VUV light and stable operability at cryogenic temperatures. For eleven R11410 and seven R8520 PMTs, we measured the relative photo-detection sensitivity at 470 nm as a function of the position of the incident light on the photocathode. Considering 80% of the photocathode surfaces, the observed non-uniformity values are in the ranges of (5–10)% and (25–30)% for the R11410 and R8520 models, respectively. We found that the non-uniformity in the inner region of the photocathode surface is dominated by light reflections on the internal components of the photosensors and that the border regions contribute dominantly to the observed non-uniformity.

**KEYWORDS:** Photomultiplier tube; Photo-detection sensitivity; Dark Matter detectors; Xenon; Hamamatsu; R8520; R11410.

---

\*Corresponding author: sandro@physik.uzh.ch

---

## Contents

<b>1. Introduction</b>	<b>1</b>
<b>2. Experimental description</b>	<b>2</b>
2.1 Description of the tested PMTs	2
2.2 Experimental setup	2
2.3 Data acquisition and high-luminosity method	3
<b>3. Data analysis</b>	<b>5</b>
3.1 Fingerprints of individual PMTs	5
3.2 Comparison of different PMTs	6
<b>4. Conclusion</b>	<b>8</b>

---

## 1. Introduction

Photomultiplier tubes (PMTs) are commonly used as photosensors in particle physics experiments due to their high quantum efficiency (QE), fast timing characteristics, low dark current and single-photon sensitivity. Dark matter search experiments using liquid xenon as the scattering target employ arrays of PMTs, exploiting their stable operation in cryogenic environments [10]. The distribution of the observed VUV scintillation light in the PMT arrays is used to reconstruct the event vertex. Generally, PMTs may show a non-uniform response depending on the hit position of the incident light on the photocathode. The event position reconstruction relies on the individual PMT response, hence an accurate characterisation of the PMTs is required. This may include the dependency of the sensitivity on the location of the photoelectron emission.

This article describes the Hamamatsu R11410 (a 3-inch diameter, circular PMT) and the R8520 (a square 1-inch PMT) [1, 2]. They are designed to feature low radioactivity levels and optimised for the operation in direct dark matter detection experiments using liquid xenon. They show a high QE at the scintillation wavelength of xenon, which lies in the vacuum ultraviolet (VUV) region at 175 nm. The R11410 is employed in the PandaX [3] and in the XENON1T [4] detectors. Furthermore it will also be installed in next-generation dark matter experiments, such as LZ [5] and XENONnT. The R8520 PMT was employed in the XENON10 [6], XENON100 [15, 7] and PandaX detectors, as well as in XENON1T and LZ for the surrounding xenon region.

The high relevance of characterising these PMTs already lead to a vast variety of studies and measurements. The general performance of the R11410 is covered in [9], its performance in cryogenic xenon environments in [10], and its intrinsic radioactivity was evaluated in [11]. Its quantum efficiency was measured by [12], and the wavelength-dependent double photoelectron emission by [13].

This work aims to improve upon existing measurements of the position dependent sensitivity of these PMTs. While [2, 9] measured the photocathode current, we used a different approach and in addition, we increased the spatial resolution of the measurements. A position-dependent PMT response was observed, as a combined effect from the QE, the collection efficiency (CE) and the inner light reflections on the internal components of the tubes. The measured *relative photo-detection sensitivity* values were normalised to the maximum measured value for each PMT. In section 2, we give a brief description of the PMTs and introduce the experimental setup used in this work. The analysis and the results of the performed measurements are presented in section 3. Section 4 summarises the main findings and provides an outlook.

## 2. Experimental description

In this section we first give a short description of the tested PMTs. It is followed by a description of the experimental setup operated at the University of Zürich to quantify the cathode uniformity of two models of Hamamatsu PMTs.

### 2.1 Description of the tested PMTs

The Hamamatsu R11410 is a photomultiplier tube with a circular 3-inch diameter window [1, 2], as shown in Figure 1. It is specifically designed for low temperature operation (down to  $-100^{\circ}\text{C}$ ) such as in liquid xenon. The wavelength-dependent quantum efficiency (QE) of its bialkali photocathode has a local maximum of  $\sim 30\%$  at 175 nm [9], the scintillation wavelength of xenon. The PMT window, made of synthetic silica, is transparent at this wavelength. The photoelectron collection efficiency (CE) on the first dynode is about 90 % [9, 11]. The bias voltage is around 1500 V, with the maximum being 1750 V [10]. At 1500 V the 12-dynode PMT has an average gain of  $5 \times 10^6$ . It consists of a cobalt free Kovar metal body of 11.4 cm length and a maximal (minimal) diameter of 7.8 cm (5.3 cm). The photocathode has a minimum effective diameter of 6.4 cm.

The Hamamatsu R8520 is a photomultiplier with a square 1-inch window [1, 2] (see Figure 1). The bialkali photocathode has a spectral response from 160 to 650 nm wavelength with a quantum efficiency of 30 % [14] at 175 nm. The 10-dynode PMT with a typical gain of  $2 \times 10^6$  [15] and dimensions of  $25.7 \times 25.7 \times 28.2 \text{ mm}^3$  has an active area of the photocathode of  $20.5 \times 20.5 \text{ mm}^2$ . The voltage applied between anode and cathode is around 800 V, with the maximum of 900 V [14].

### 2.2 Experimental setup

The measurements, as presented in the following sections, were performed at room temperature in a light-tight black box which can accommodate four R11410 PMTs fixed in Acrylonitrile Butadiene Styrene holders. Adapters can be inserted into the holders to fix an R8520 PMT. The custom-made experimental setup (*SandBox*) which was used for the measurements, is shown schematically in Figure 2 and described in detail in [16]. A collimated light source fixed on a two-axis scanner can be controlled from the outside to move in a plane parallel to the photocathode with a maximal spatial resolution of  $15 \mu\text{m}$ . The light source consists of a black anodised light tight aluminium box containing a blue, 470 nm wavelength, LED covered with a collimator plate. The collimation of the beam is performed by two aligned apertures separated by a small gap. The apertures used for the presented measurements have 0.5 mm diameter. The distance between the collimator and the

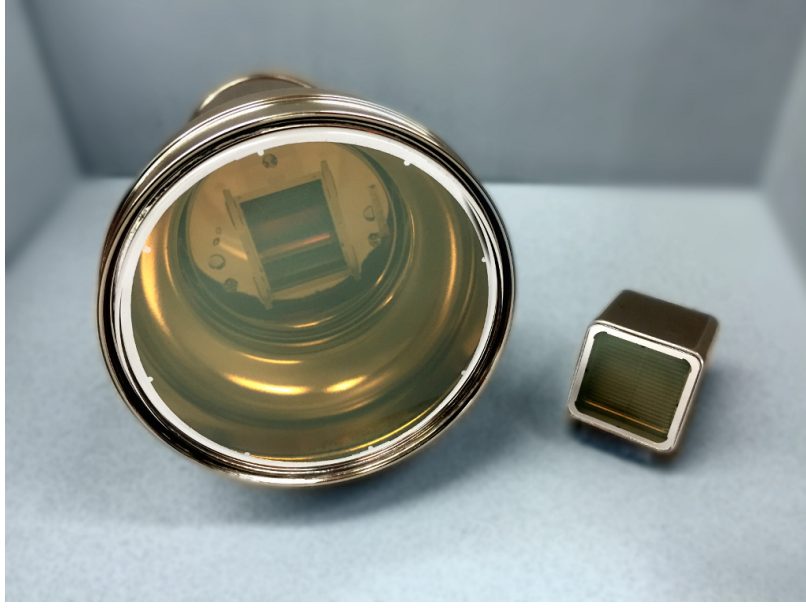


Figure 1: (Left): Front view of a Hamamatsu R11410 PMT with visible inner structure (focusing dynode, first dynode and metal screws). (Right): View of a Hamamatsu R8520 PMT with visible first dynode stage.

PMT window is set to 1 mm. This results in an enlightened pixel diameter of 0.7 mm on the photocathode. In order to perform the measurements in a stable and reproducible configuration, they were started not earlier than 60 minutes after switching on the PMTs. The temperature inside the black box was monitored during the measurements: due to the strong thermal insulation of *Sand-Box*, achieved by 4 mm thick tar paper on the inner walls, the observed temperature fluctuations are lower than 0.5 degrees.

### 2.3 Data acquisition and high-luminosity method

To measure the photo-sensitivity uniformity, the emission of photoelectrons is stimulated by illumination of the photocathode at different positions with collimated light from an LED of 470 nm wavelength. A pulse generator (Telemeter TG4001) is used to bias the LED and to simultaneously trigger the data acquisition. With the high-luminosity (HL) method the light intensity is chosen such that 100% of the events provide a signal used to determine the photocathode sensitivity ( $\sim 600$  photoelectrons). A signal pulse is defined as a charge signal larger than  $3 \times \text{RMS}$  of the baseline. The light source is fixed on a computer-controlled XY-scanning table [16], that is moved between each measured pixel to scan the entire surface of the photocathode. The data presented here are acquired using a CAEN V1724 waveform digitizer with 100 MHz sampling frequency and 40 MHz input bandwidth. The employed voltage dividers are identical to those used in XENON100 and XENON1T, and are described in detail by [17]. The trigger frequency is 4 kHz. The waveforms are transferred to a computer and stored for data processing and subsequent analysis, as well as for visual inspection. A peak processor software scans the digitised waveforms for excursions of 3 times the RMS from the baseline, integrates the area to obtain the number of electrons contributing to the signal, and histograms the result in a spectrum. The integration window starts when the excursions exceed the defined threshold and ends when the threshold is undercut. Figure 3 shows

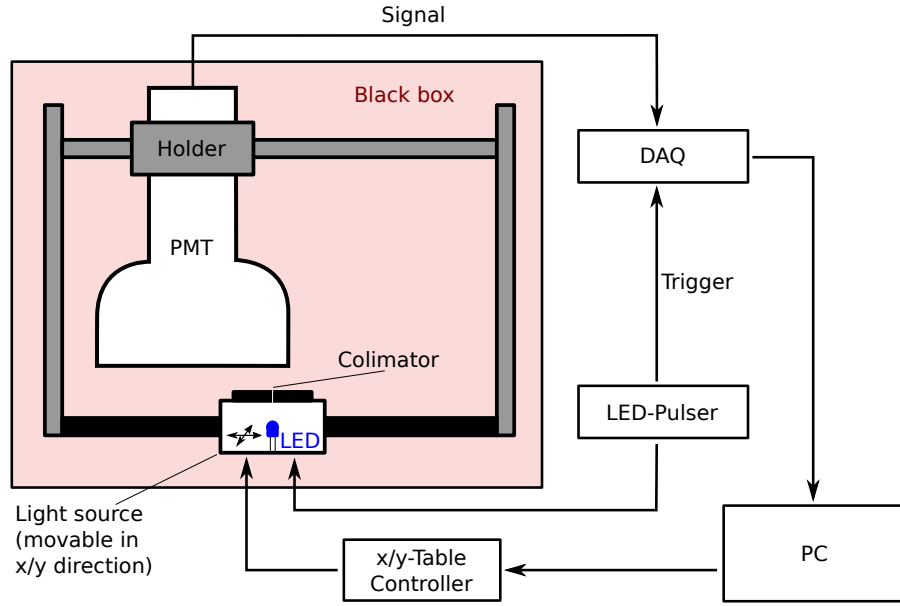


Figure 2: Schematic view of the experimental setup, *SandBox*. The XY-table with the light source and a 0.5 mm collimator are inserted into the blackbox, and a PMT with its voltage divider is installed into a holder.

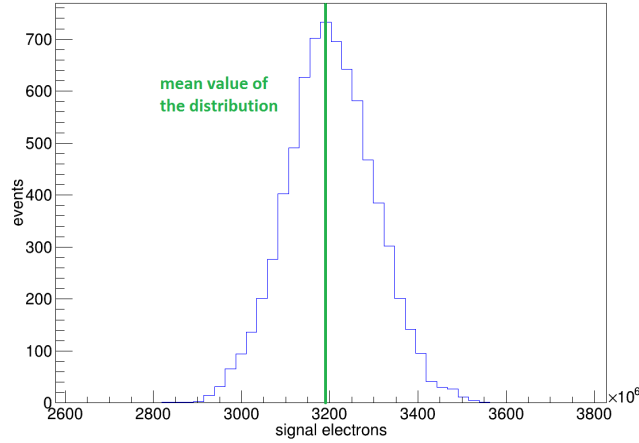


Figure 3: An example of a high-luminosity spectrum of a R11410 PMT. The green vertical line corresponds to the mean value of the the total detected light for one pixel during one measurement.

an example of such an high-luminosity spectrum of a R11410 PMT. The mean of the distribution is proportional to the number of detected photoelectrons, and hence to the sensitivity of the illuminated spot of the photocathode. This value thus defines the sensitivity of the given spot, with the highest measured value on the PMT defining 100% relative sensitivity.

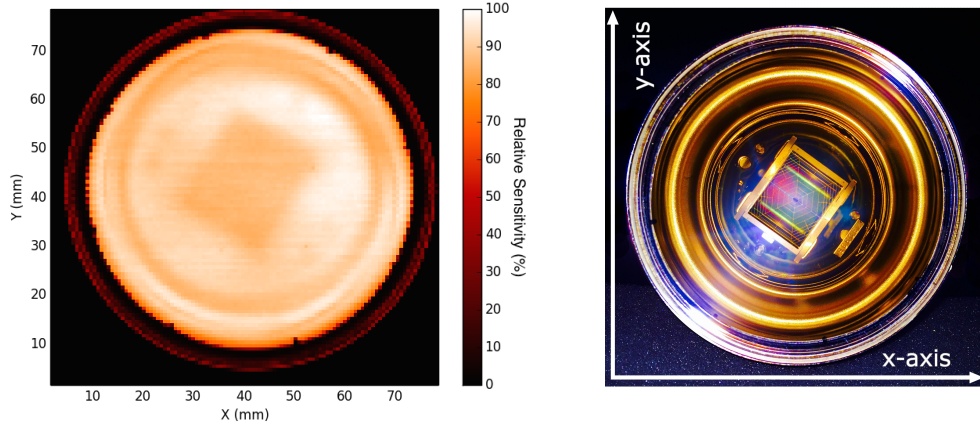


Figure 4: (Left): Planar relative sensitivity of the photocathode of a R11410 PMT normalised by the highest measured value obtained with the high luminosity method. A total of 9779 pixels were scanned. (Right): Front view of a R11410 PMT with visible inner structure (focusing dynode, first dynode and screws).

### 3. Data analysis

The result of each analysis can be visualised as a two-dimensional map of relative sensitivities (each normalised by the pixel with the highest sensitivity), a so-called *fingerprint*.

The non-uniformity is defined by the standard deviation of all pixels in the fingerprint

$$s = \sqrt{\frac{1}{n-1} \sum_i^n (x_i - \bar{x})^2}, \quad (3.1)$$

where  $n$  is the number of pixels,  $x_i$  is the mean value of the high luminosity spectrum for the pixel  $i$ , and  $\bar{x}$  is the average value of all pixels in the selected area.

#### 3.1 Fingerprints of individual PMTs

In Figures 4 and 5 the fingerprints of a R11410 and a R8520 PMT are shown with a pixel distance of 0.7 mm, for a total of 9779 and 4918 scanned pixels, respectively. For each point,  $10^4$  events were acquired. The scanning of an R11410 PMT takes 25 hours. The unique properties of each fingerprint are preserved when the PMTs are rotated and rescanned, hence the non-uniformity is not biased by the apparatus.

For the R11410 PMT, the inner structure of the PMT, shown in Figure 4 (left), becomes visible in the fingerprint. This is due to a fraction of incident photons that are not absorbed in the photocathode and penetrate into the inner volume of the PMT, where they are reflected on metal surfaces. These photons may hit the photocathode from the rear side and produce a photoelectron. However, the magnitude of the effect depends on the reflectivity of these components to the 470 nm light. Since the light from the LED is collimated and hence penetrates the PMT almost perpendicular to the photocathode, the effect is position-dependent. Pixels with a high reflecting background – such as blank flat metal surfaces – increase the sensitivity of the PMT at that position, while pixels with lower reflecting background – such as screw heads (for example,  $(x, y) = (23 \text{ mm}, 45 \text{ mm})$ )



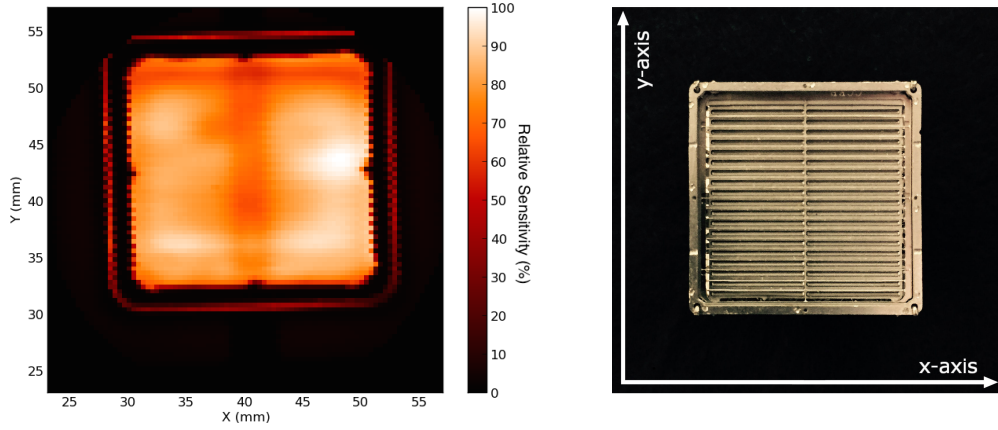


Figure 5: (Left): Planar relative sensitivity of the photocathode of a R8520 PMT normalised by the highest measured value obtained with the high luminosity method. A total of 4918 pixels were scanned. (Right): Front view of an opened R8520 PMT. The T-shaped holding structure and the first dynode stage are clearly visible.

in Figure 4), or the region of the focusing grid and the first dynode in the center – show a decreased sensitivity. From this measurement, it can be concluded that the dominant variation of the photocathode uniformity is caused by the reflections of the photons on inner PMT components.

The inner structure of the R8520 PMT also becomes visible in the fingerprint. On every dynode, a T-shaped holding structure is fixed and decreases the sensitivity of the PMT at this position (see Figure 5). It can be explained by the fact that some of the incident photons get poorly reflected at the welding site and some of the emitted electrons from the photocathode are collected on the welding line instead of the first dynode stage. Due to the absence of a focusing dynode, the photo-electrons can be collected at different positions on the first dynode stage. This results in a position-dependent electron collection efficiency, and hence in regions on the fingerprint that show higher and lower sensitivity.

### 3.2 Comparison of different PMTs

Eleven R11410 PMTs and seven R8520 PMTs were systematically scanned using the HL method. Figure 6 shows the radial dependency for the 3-inch PMTs (left) and the dependency projected along the y-axis of the 1-inch PMTs (right) of the relative sensitivity. For the 3-inch PMTs, the curves show the average of all measured pixels at a particular radius, while for the 1-inch PMTs the average is calculated at a particular x-position of each PMT. The 3-inch PMTs show a maximum efficiency value at a radius of about 17 mm. At the center, the photo-detection efficiency is on average 7% lower. For larger radii, there is a larger difference in the trend for different 3-inch PMTs, but the efficiency of all PMTs decreases for a radius larger than  $\sim 30$  mm. One side of the 1-inch PMTs is on average 10% more sensitive than the other. The central region shows a decreased sensitivity of about 10% with respect to the most sensitive border. To quantify the non-uniformity for a given PMT, a certain area on the photocathode is selected. We use three different selections, as shown in Figure 7, namely 60%, 80% and 90% of the total area.

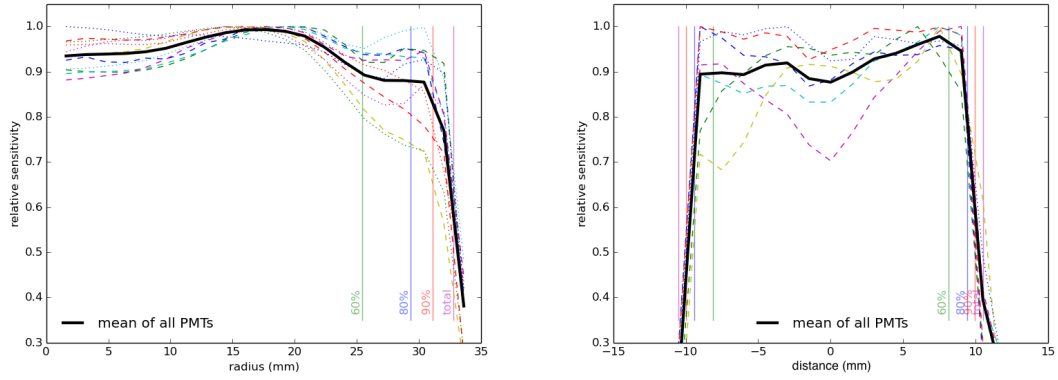


Figure 6: Average relative photo-detection sensitivity (normalised to the maximum value of each PMT) of all pixels at a given radius of eleven R11410 PMTs (left), and average photo-detection sensitivity projected along the y-axis of seven R8520 PMTs (right): The solid black curve indicates the average for the scanned PMTs. Thin vertical solid lines mark the radii for 60% (green), 80% (blue), 90% (red) of the area, as well as for the total sensitive PMT area (magenta).

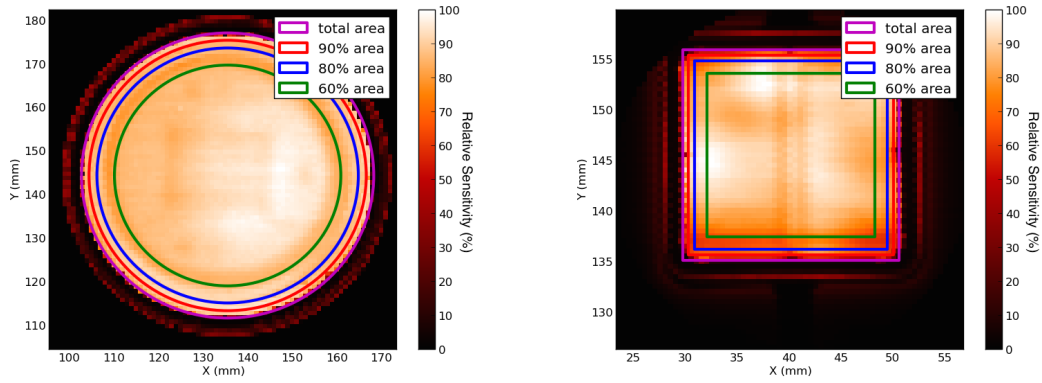


Figure 7: Different radial or squared selection cuts for 60% (green), 80% (blue), 90% (red) of the area, and the total PMT area (magenta). Show are a circular R11410 PMT (left) and a square R8520 PMT (right).

Figure 8 shows the non-uniformity values for all scanned PMTs for the three different area selections. In general, the R11410 sensors show a higher uniformity, even when going to larger areas, whereas the R8520 PMTs change their uniformity drastically when we take into account pixels near the sensor edges.

Four of the R11410 PMTs (samples 1, 2, 7, and 10) show an excellent uniformity within 60% of the photocathode area. For these PMTs, the uniformity indeed does not vary much when the selected area is increased: for all 3 shown area selections, the measured non-uniformity is less than 5%. The photo-sensitivity non-uniformity of four PMTs (samples 3, 4, 5, and 9) is small for 60% of the area, namely around 5%, however it increases for larger areas, up to 10%. Three of the PMTs (samples 6, 8, and 11) have a rather high non-uniformity when selecting 60% of the area, about 9%. This value increases to 14% when 90% of the photocathode area is considered.



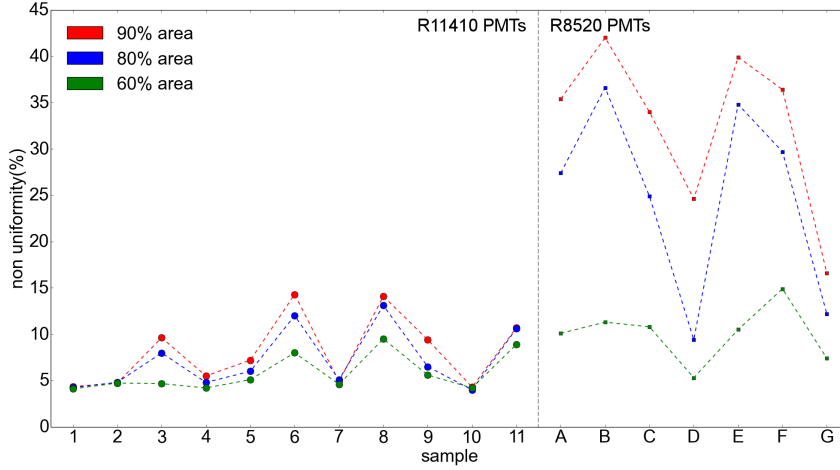


Figure 8: Non-uniformity values for different active areas on the photocathodes, 90% (red), 80% (blue) and 60% (green), of eleven R11410 PMTs (samples 1-11) and seven R8520 PMTs (samples A-G).

Considering 60% of the photocathode area, the R8520 PMTs show a non-uniformity of about 10%, which is slightly higher than for the R11410 PMTs. For 90% of the area, the non-uniformity is between 35% and 40%. However, two PMTs (samples D and G) show a better non-uniformity of about 6% and 20% for 60% and 90% of their areas, respectively.

#### 4. Conclusion

We measured the relative photo-detection sensitivity at 470 nm for eleven Hamamatsu R11410 and seven R8520 PMTs, and thus quantified the non-uniformity of their photocathodes. For the 3-inch, R11410 sensors, interesting features were observed: their semi-transparent photocathode is penetrated by a fraction of the photons that may then be reflected on structural parts inside the PMT towards the photocathode, where they produce a photoelectron. Hence the observed non-uniformity is dominated by the reflectivity of the structural components behind the photocathode. We observed that the non-uniformity is stronger at the edges of the photocathode surface than at the center region. For the R8520 PMTs, we observed that their response is less uniform, most likely due to the absence of a focusing dynode stage. This effect could be further investigated by simulating the photoelectron paths inside the PMT. Using the non-uniformity value as a quality requirement for the photosensors leads to the conclusion that the 3-inch PMTs show a superior behaviour than the 1-inch sensors.

In dark matter detectors using liquid xenon as target, event vertex reconstruction is performed by computer algorithms which so far assume a perfectly uniform photocathode sensitivity (see for example XENON100 [15]). A systematic study of all the PMTs employed in such a detector could potentially improve the uncertainty in event position reconstruction by taking into account the position-dependent sensitivity of each sensor. However, since the xenon scintillation light has a wavelength of 175 nm, the study must be extended to investigate the photo-sensitivity for VUV light. This could be achieved in a similar setup as we described, by using a VUV light source.

## References

- [1] <http://www.hamamatsu.com>
- [2] Hamamatsu photonics K.K. *Photomultiplier Tubes – Basics and Applications* (third edition 2007)
- [3] Mengjiao Xiao et al. *First dark matter search results from the PandaX-I experiment Sci China-Phys Mech Astron* **57**, 2024-2030 (2014) arXiv:1408.5114 [hep-ex]
- [4] E. Aprile, et al. *The XENONIT Dark Matter Search Experiment*, arXiv:1206.6288 [astro-ph-IM] (2012).
- [5] D.C. Mallin et al. *After LUX: The LZ Program* arXiv:1110.0103 [astro-ph.IM]
- [6] J.Angle, et al. *A search for light dark matter in XENON10 data. Phys. Rev. Lett.* **107**, 051301 (2011) arXiv:1104.3088 [astro-ph.CO]
- [7] E. Aprile et al. *Dark matter results from 225 live days of XENON100 data. Phys. Rev. Lett.* **109**, 181301 (2012) arXiv:1207.5988 [astro-ph.CO]
- [8] E. Aprile et al. *Response of the XENON100 Dark Matter Detector to Nuclear Recoils Phys. Rev. D* **88**, 012006 (2013) arXiv:1304.1427 [astro-ph.IM]
- [9] K. Lung et al. *Characterization of the Hamamatsu R11410-10 3-inch photomultiplier tube for liquid xenon dark matter direct detection experiments NIM. A.* **696**, 32-39 (2012) arXiv:1202.2628 [physics.ins-det]
- [10] L. Baudis et al., *Performance of the Hamamatsu R11410 photomultiplier tube in cryogenic xenon environments 2013 JINST* **8** P04026 arXiv:1303.0226
- [11] D.S. Akerib, *An ultra-low background PMT for liquid xenon detectors NIM. A* **703**, 1-6 (2013) arXiv:1205.2272
- [12] A. Lyashenko et al., *Measurement of the absolute Quantum Efficiency of Hamamatsu model R11410-10 photomultiplier tubes at low temperatures down to liquid xenon boiling point 2014 JINST* **9** P11021 arXiv:1410.3890
- [13] C. H. Faham et al., *Measurements of wavelength-dependent double photoelectron emission from single photons in VUV-sensitive photomultiplier tubes* arXiv:1506.08748
- [14] E. Aprile et al. *Measurements of the quantum efficiency of Hamamatsu R8520 photomultipliers at liquid xenon temperature 2012 JINST* **7** P10005 arXiv:1207.5432v1 [astro-ph.IM]
- [15] E. Aprile et al. *The XENON100 Dark Matter Experiment Astropart. Phys.*, **35**, 573-590 (2012) arXiv:1107.2155 [astro-ph.IM]
- [16] Sandro D’Amato, Bachelor of Science thesis, *SandBox: A facility for XENON photosensors characterization and measurements of photocathode uniformity*, University of Zurich, Switzerland (2014) [http://www.physik.uzh.ch/groups/groupbaudis/darkmatter/theses/xenon/bachelor\\_damato.pdf](http://www.physik.uzh.ch/groups/groupbaudis/darkmatter/theses/xenon/bachelor_damato.pdf)
- [17] Annika Behrens, Dissertation, *Light Detectors for the XENON100 and XENONIT Dark Matter Search Experiment*, University of Zurich, Switzerland (2014) [http://www.physik.uzh.ch/groups/groupbaudis/darkmatter/theses/xenon/thesis\\_behrens.pdf](http://www.physik.uzh.ch/groups/groupbaudis/darkmatter/theses/xenon/thesis_behrens.pdf)